

The Green function for potential flow in a rectangular channel

J.N. NEWMAN

Department of Ocean Engineering, Massachusetts Institute of Technology, Cambridge, MA 02139, USA

Abstract. The evaluation of the Green function is considered for the three-dimensional Laplace equation, in the interior of a rectangular channel subject to homogeneous Neumann conditions on the boundaries. To complement the Fourier eigenfunction expansion which is effective in the far-field, a near-field algorithm is developed based on the simpler Green function for a channel of infinite width, using images to account for the channel sides. Examples are given of numerical applications including the added mass of a sphere in a square channel, and the interaction force between a ship and an adjacent canal wall.

1. Introduction

Three-dimensional potential flows inside rectangular channels are of interest in various applications. These include wall corrections in water- and wind-tunnels, and problems associated with ships moving in canals. In the latter case, if the Froude number is sufficiently small, wave effects are negligible and the free-surface condition can be replaced by a homogeneous Neumann boundary condition. In applications where Dirichlet boundary conditions are applicable the corresponding Green functions can be derived by superposition of appropriate pairs of the functions considered here, with opposite signs.

The Green function for a rectangular channel can be constructed simply from the free-space singularity $1/r$ and a doubly-periodic array of images. This representation is useful conceptually, but the very slow convergence of the doubly-infinite series makes it unsuitable for routine computations. Alternative representations have been derived by Breit [1]. One, reproduced below as equation (7), is an eigenfunction expansion involving trigonometric functions of the coordinates transverse to the channel axis, and exponential functions of the axial coordinate. This expansion is simple and effective if the axial distance between the source and field points is moderate or large compared to the *larger* of the two transverse dimensions of the channel, the width w or height h . To complement this representation Breit derives an elegant Taylor series expansion of the images about the source point. Since the radius of convergence is limited by the distance to the nearest image, one expects this series to be useful computationally in a spherical domain with radius of the order of the *smaller* dimension of the channel. Thus for channels where h and w are substantially different, the two complementary expansions given in [1] do not suffice.

A simpler analysis applies in the limits $w/h \rightarrow \infty$ or $w/h \rightarrow 0$, which are fundamentally identical except for scaling and definition of the coordinates. For definiteness we consider the former case, corresponding to the domain between two parallel horizontal planes which are unbounded. The Green function can be constructed from a single periodic array of images, situated on the vertical axis above and below the source point. The potential is axisymmetric about this axis. The eigenfunction expansion involves trigonometric functions of the axial coordinate, and modified Hankel functions K_0 in the radial coordinate R . This expansion is efficient for large or moderate values of R , relative to the height h between the two

boundaries. For smaller values of R/h a Taylor series has been derived by Breit [1], and Newman [2] has developed Chebyshev expansions and economized polynomials. The latter representation permits computation of the singly-periodic Green function with single-precision accuracy for $R < h$ with only 21 polynomial coefficients. In the complementary domain $R > h$ the eigenfunction expansion requires only six terms for single-precision accuracy, and thus the computation of the singly-periodic Green function is effectively achieved by these two complementary algorithms. An important feature of this Green function is its logarithmic behaviour for $R \gg h$, a consequence of the fact that at large radial distances the array is equivalent asymptotically to a two-dimensional line source.

In the present work the Green function for an arbitrary rectangular channel is constructed by periodic superposition of the simpler infinite-width Green functions, along the transverse axis normal to the channel sides. In its original form this representation is slowly convergent, due to the logarithmic component noted above, but this can be summed separately with a closed-form potential equivalent to an array of two-dimensional sources. The remainder, associated with the modified Bessel functions in the eigenfunction expansion, converges exponentially. Examples are given of computations based on this approach including the added mass of a sphere in a square channel, and the analysis of the bank-interaction force for a ship moving in a canal.

2. Analysis

A rectangular channel of width w and height h is considered, with unbounded length. Without loss of generality it can be assumed that $w \geq h$. Nondimensional coordinates are defined in terms of the height h , which is assumed hereafter to be equal to one. Thus the interior of the channel is the three-dimensional space $(-\infty < x < \infty, 0 < y < w, 0 < z < 1)$, where $w \geq 1$. The desired Green function $G(x - \xi, y, \eta, z, \zeta)$ is the potential of a source, situated at the point ξ, η, ζ inside the channel and subject to homogeneous Neumann boundary conditions on these boundaries. The governing equation is

$$\nabla^2(G - 1/r) = 0, \quad (1)$$

where $1/r = [(x - \xi)^2 + (y - \eta)^2 + (z - \zeta)^2]^{-1/2}$ is the free-space Green function in the absence of the channel boundaries. The boundary conditions take the form

$$\partial G / \partial y = 0, \quad \text{on } y = 0, w, \quad (2)$$

$$\partial G / \partial z = 0, \quad \text{on } z = 0, 1. \quad (3)$$

Any linear function of x with constant coefficients is a homogeneous solution of (1–3), corresponding physically to a uniform streaming flow through the channel. To eliminate such a component it is appropriate to impose the far-field condition

$$G = U|x| + o(1), \quad \text{for } |x| \rightarrow \infty. \quad (4)$$

This states that the flux from the source is equally divided between $\pm\infty$, with limiting velocities $\pm U$. Since the singularity $1/r$ corresponds to a source with a flux -4π , the

constant $U = -2\pi/w$ is specified by continuity. (The singularity corresponds more precisely to a *sink*, but the more general term *source* is retained here with the understanding that its strength is negative.) The far-field condition (4) also fixes the value of the arbitrary constant in the solution of (1-3).

A formal solution can be constructed by superposition of four simpler functions,

$$G(x - \xi, y, \eta, z, \zeta) = G_0(x - \xi, y - \eta, z - \zeta) + G_0(x - \xi, y + \eta, z - \zeta) \\ + G_0(x - \xi, y - \eta, z + \zeta) + G_0(x - \xi, y + \eta, z + \zeta), \quad (5)$$

where $G_0(x, y, z)$ is defined by (1-4) with the source point at the origin ($\xi = 0, \eta = 0, \zeta = 0$). The function G_0 corresponds to a doubly-periodic array of free-space Green functions, situated at the points $x = 0, y = 2mw, z = 2n$, where the integers m, n take all positive and negative values as well as zero. The solution of (1-4) can thus be constructed from (5) with a basic potential of the form

$$G_0 = \frac{1}{r} + \sum_{m=-\infty}^{\infty} \sum_{\substack{n=-\infty \\ |m|+|n|>0}}^{\infty} \{[x^2 + (y + 2mw)^2 + (z + 2n)^2]^{-1/2} - [(2mw)^2 + (2n)^2]^{-1/2}\} + C. \quad (6)$$

Here the extra inverse square-root is a constant, subtracted from each term to secure convergence. The additional constant C is required to satisfy (4). (In [1] the unknown constant is included in (4), instead of (6). Since we do not use (6) directly in our analysis the present convention is more convenient.)

The series (6) is unsuitable for numerical applications, due to its very slow convergence. A more useful computational form can be derived by Fourier techniques, as in [1], with the result

$$G_0 = -\frac{\pi|x|}{2w} + \frac{\pi}{2w} \sum_{m=0}^{\infty} \sum_{\substack{n=0 \\ m+n>0}}^{\infty} \varepsilon_m \varepsilon_n \frac{\cos u_m y \cos v_n z}{(u_m^2 + v_n^2)^{1/2}} e^{-\sqrt{u_m^2 + v_n^2}|x|}, \quad (7)$$

where

$$\varepsilon_0 = 1, \quad \varepsilon_m = 2 \quad \text{for } m \geq 1,$$

$$u_m = m\pi/w, \quad v_n = n\pi.$$

Note that the far-field condition (4) is satisfied without introducing an additional constant. This expansion is simple to evaluate and rapidly convergent, provided $|x| \geq O(w)$.

As the basis for effective numerical algorithms in the complementary domain $|x| \leq O(w)$, we consider a single periodic array, equivalent to the contribution with $m = 0$ in (6) except for a constant, and defined by the series expansion

$$g(R, z) = [R^2 + z^2]^{-1/2} + \gamma - \log 4 + \sum_{\substack{n=-\infty \\ n \neq 0}}^{\infty} \left\{ [(R^2 + (z + 2n)^2)^{-1/2} - \frac{1}{2|n|}] \right\}. \quad (8)$$

Here $R = (x^2 + y^2)^{1/2}$ is the radial distance from the array axis, and $\gamma = 0.577 \dots$ is Euler's

constant. Equation (8) defines a periodic function of z , which can be expanded in a Fourier series, as in Gradshteyn & Ryzhik [3, §8.526]. The resulting expression is

$$g(R, z) = -\log R + 2 \sum_{n=1}^{\infty} \cos(n\pi z) K_0(n\pi R), \quad (9)$$

where K_0 is the modified Hankel function. Since K_0 is exponentially small for large values of its argument the series in (9) converges rapidly if $R \gg O(1)$. For large values of R

$$g(R, z) = -\log R + O(R^{-1/2} e^{-\pi R}). \quad (10)$$

The first term in (9) is a two-dimensional source; the asymptotic approximation (10) is equivalent to the statement that the array of three-dimensional point sources appears in its far field as a simple line source with the same total flux.

Returning now to the case of the doubly-periodic array (6), our plan is to construct this function by summation of the single array g and its images. Except for the term $\log R$, the asymptotic approximation (10) confirms the convergence of such a procedure. We therefore consider the modified series

$$G_0(x, y, z) = G_{2D}(x, y) + \sum_{m=-\infty}^{\infty} [g(R_m, z) + \log R_m], \quad (11)$$

where $R_m = [x^2 + (y - 2mw)^2]^{1/2}$, and

$$\begin{aligned} G_{2D}(x, y) &= -\log\left(\frac{\pi R_0}{w}\right) - \sum_{\substack{m=-\infty \\ m \neq 0}}^{\infty} \log\left(\frac{R_m}{2|m|w}\right) \\ &= -\operatorname{Re} \log 2 \sinh \frac{\pi(x + iy)}{2w} = -\frac{1}{2} \log\left(2 \cosh \frac{\pi x}{w} - 2 \cos \frac{\pi y}{w}\right). \end{aligned} \quad (12)$$

The function G_{2D} is the potential of a two-dimensional periodic array of sources. Except for a constant, the evaluation of the series in (12) can be confirmed by differentiation with respect to the complex variable $(x + iy)$. The constant is evaluated by considering the limit of (12) for $x + iy \rightarrow 0$. Finally, from the last expression in (12), it follows for large $|x|$ that

$$G_{2D} = -\frac{\pi|x|}{2w} + O(e^{-\pi|x|/w}). \quad (13)$$

Since each term in the infinite series of (11) is exponentially small, in accordance with (10), it follows that the asymptotic approximation (13) also applies to G_0 , confirming the far-field form of the latter function and the constants in (11) and (12).

The validity of (11) can be confirmed directly. The function G_{2D} satisfies the boundary conditions (2), and each term satisfies (3). The boundary conditions (2) are satisfied by the sum in (11) as a result of periodicity and symmetry. Since the logarithmic singularities in the first and last terms cancel, the only remaining singularity within the channel domain is the contribution from the first term on the right-hand-side of (8), in the term $m = 0$ of (11), which is precisely the three-dimensional source singularity $1/r$ associated with the Green function. Thus all of the prescribed conditions (1–4) are satisfied by (11).

3. Numerical procedure

Three algorithms are effective collectively in the evaluation of the Green function G . The simplest, based on (7), is straightforward to implement. A maximum of eight terms in each series is sufficient to give 6D accuracy in the domain $|x|/w > 0.6$. In the complementary domain the series (11) can be utilized, with the single array g evaluated in the manner to be described below.

For arbitrary points within the domain of the channel, the radius R_m to the m th image in (11) is greater than or equal to the lower bound $2|m|w - 1$. For large values of $|m|$ the terms in (11) are exponentially small, in proportion to the factors $\exp(-2\pi|m|w)$. Since $w \geq 1$ the series in (11) can be summed numerically with rapid convergence. Eight terms ($-3 \leq m \leq 4$) are required for 6D accuracy. With the exception of the term $m = 0$, $R_m \geq w \geq 1$, and the summands in (11) can be evaluated effectively from (9).

A complementary algorithm can be employed to evaluate the term $m = 0$ if $R_0 < 1$, based on the two-dimensional Chebyshev expansions and economized polynomials presented in [2], with the result

$$g(R, z) \approx [R^2 + z^2]^{-1/2} + [R^2 + (z + 2)^2]^{-1/2} + [R^2 + (z - 2)^2]^{-1/2} + \sum_{m,n} a_{mn} R^{2m} z^{2n}. \quad (14)$$

Using the coefficients in Table 1, this economized polynomial approximation is accurate in ($0 \leq R \leq 1$, $0 \leq z \leq 1$), to about 8 decimals. (Except for the constant a_{00} , the entries in Table 1 are identical to Table 2 of [2].)

When $R_0 < 1$ it is advisable to cancel the term $\log R_0$ in the series (11) with the corresponding singular term of (12). Note that $G_{2D} + \log R_0$ is a regular function of (x, y) in $0 \leq y \leq w$, but care is required to evaluate this sum robustly when both x and y tend to zero.

When one or more of the square-root singularities in (14) is large, it is advisable to subtract these terms from G and evaluate their contributions in the usual manner of treating the free-space Green function in a boundary integral equation.

4. Applications

The Green function described in the preceding sections has been combined with a three-dimensional panel code based on Green's theorem. This code, a derivative of the free-surface radiation/diffraction program WAMIT, assumes flat quadrilateral panels and constant values of the unknown potential, or source strength, on each panel. An iterative solver is used for the linear system to permit relatively large numbers of panels, and corresponding

Table 1. Coefficients a_{mn} in the economized polynomial approximation (14)

n	$m = 0$	$m = 1$	$m = 2$	$m = 3$	$m = 4$
0	-1.80907870	-0.02525711	0.00086546	-0.00004063	0.00000193
1	0.05051418	-0.00692380	0.00073292	-0.00006636	0.00000398
2	0.00230838	-0.00097875	0.00020597	-0.00003333	0.00000524
3	0.00012934	-0.00010879	0.00003965	-0.00000891	
4	0.00000913	-0.00001270	0.00000466		

unknowns, on the body surface. Two simple applications are described here to illustrate the utility of the channel Green function. More complicated applications are described in [4], involving the interactions between two ships where one is moving past the other in a canal.

In the first application we consider the added mass of a sphere, of diameter D , centered in a square channel of width w and height $h = w$. The added-mass coefficients are defined by the integrals

$$a_{ij} = \rho \iint \phi_j n_i \, dS. \quad (15)$$

Here ρ is the fluid density, ϕ_j is the velocity potential for motion of the body in the direction j with unit velocity, and n_i is the component of the unit normal vector in the direction i . (Rotational modes and moments can be considered by straightforward extensions of these definitions.) The integral in (15) is over the body surface. Due to the spherical geometry of the body, with its center on the axis of the channel, a_{11} , a_{22} and a_{33} are the only non-zero elements of the matrix a_{ij} . Since the channel is square, $a_{22} = a_{33}$. In an unbounded fluid, corresponding to the limit $D/w = 0$, these coefficients are equal to one-half of the displaced fluid volume. In the presence of the channel walls a_{11} and $a_{22} = a_{33}$ have different values which depend on D/w .

To test for convergence three discretizations of the sphere are used, with a total of $N = 128, 512, 2048$ panels. (In the computations one plane of symmetry is imposed, reducing the total number of unknowns to half of these numbers. Two or three planes of symmetry could be utilized with additional programming effort.) Computations have been performed with $D/w = 0(.05)1.0$ for each of the three discretizations. In the limit $D/w = 0$ only the $1/r$ free-space Green function is considered. The complementary limit $D/w = 1$ is non-physical, corresponding to the case where the sphere is tangent to the channel boundaries.

The results are listed in abbreviated form in Table 2, which also includes extrapolated values for $N = \infty$ based on Richardson extrapolation. The effectiveness of this extrapolation is confirmed by noting that in all cases, including the singular limit $D/w = 1$, the results of the first and second extrapolants agree to three or more significant figures. The extrapolated

Table 2. Added-mass coefficients a_{11} (upper table) and a_{22} (lower table) for a sphere of diameter D , centered in a square channel of width w

D/w	$N = 128$	$N = 512$	$N = 2048$	$N = \infty$	$N = \infty$
0.0	0.47968	0.49492	0.49874	0.50001	0.50001
0.2	0.48583	0.50157	0.50554	0.50686	0.50687
0.4	0.53041	0.54973	0.55466	0.56630	0.55631
0.6	0.66681	0.69802	0.70604	0.70871	0.70873
0.8	1.02544	1.09381	1.11177	1.11775	1.11783
1.0	2.34813	2.65608	2.74970	2.78091	2.78239
0.0	0.49018	0.49775	0.49947	0.50004	0.50002
0.2	0.49431	0.50218	0.50401	0.50462	0.50461
0.4	0.52403	0.53403	0.53637	0.53714	0.53713
0.6	0.61135	0.62785	0.63193	0.63330	0.63329
0.8	0.81811	0.85229	0.86100	0.86391	0.86392
1.0	1.39278	1.52964	1.57288	1.58730	1.58810

N denotes the total number of panels used to represent the sphere. The last two columns are based on Richardson extrapolation of the entries in the preceding two and three columns, respectively. All coefficients are normalized by the displaced mass of fluid, $\pi\rho D^3/6$.

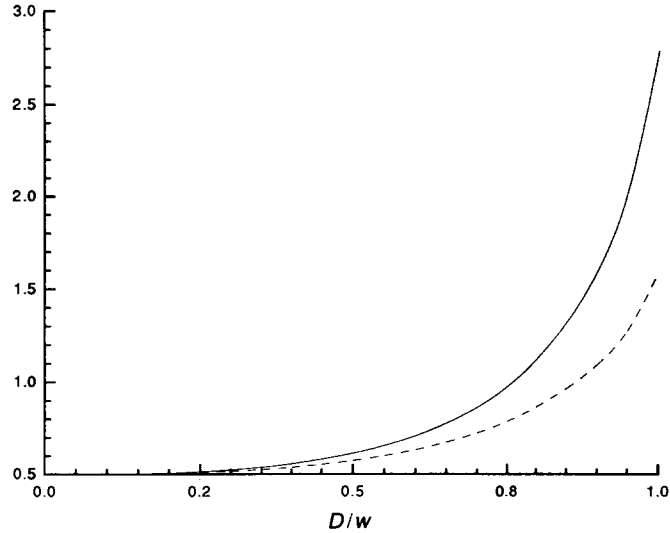


Fig. 1. Added mass of a sphere, of diameter D , in a square channel of width w , normalized by the mass of fluid displaced by the sphere. The solid curve represents the longitudinal added mass, for acceleration along the channel axis, and the dashed curve is for transverse acceleration, normal to one of the channel sides.

values are plotted in Fig. 1, as ratios of the added-mass coefficients in an unbounded fluid. The effect of the channel is to increase the added mass, particularly the longitudinal coefficient a_{11} , but the increase is small for $D/w \leq 0.5$.

As a more practical example, a ship hull is considered to move with constant velocity along rectangular canal and the same panel program is used to calculate the 'bank suction force' which acts in the transverse direction, forcing the ship toward the nearest side of the canal. The free surface is considered to be rigid and represented by a simple image, as is

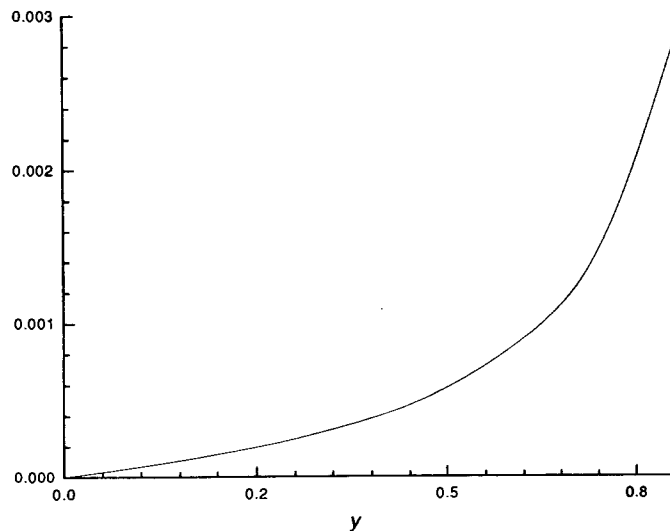


Fig. 2. Transverse 'bank-suction' force on a ship in steady translation along a rectangular canal, as a function of its transverse position y away from the canal centerline. The force is normalized by $\frac{1}{2}\rho U^2 L^2$ where ρ is the fluid density, U is the ship's velocity and L its length. The transverse position y is normalized by the half-width of the canal.

appropriate when the Froude number is small. The ship considered is a ‘Mariner’ hull form, represented by a total of 400 panels. We take the ship length to be one, giving a normalized draft of 0.057 and a half-beam of 0.073. The canal is assumed to have a unit width and a depth of 0.068. Figure 2 shows the resulting computed values of the transverse force coefficient, as a function of lateral position in the canal. The force vanishes when the ship is on the centerline, from symmetry, and increases rapidly as the ship moves toward one side of the canal.

5. Discussion

The Green function for Laplace’s equation in the domain interior to a rectangular channel, of infinite length and constant width and height, can be represented directly in terms of the doubly-periodic array of free-space Green functions $1/r$, as in (6). In the limiting case where the width (or alternatively the height) is infinite, the problem reduces to that of a single source between two parallel infinite planes, or equivalently to the singly-periodic array (8). In their direct representations (6) and (8), neither the doubly-periodic or singly-periodic arrays are sufficiently convergent to permit effective numerical evaluation.

The principal result of the present analysis is the representation (11) for the potential of the doubly-periodic array, in terms of a sum of the simpler singly-periodic array and its images. The practical value of this construction results from the analytic simplicity of the singly-periodic array. Most significantly, the logarithmic behavior of the singly-periodic array can be analysed separately and summed over the image system in closed form, corresponding in effect to a two-dimensional far-field solution in planes normal to the array axis. After subtracting this two-dimensional part, the remaining components of the image system are exponentially convergent, and can be summed directly. Another advantage of the construction in terms of the singly-periodic array is the fact that it is amenable to efficient computation, using complementary algorithms such as the eigenfunction expansion (9) and economized polynomial approximation (14).

This procedure has been tested extensively in applications to problems of ship hydrodynamics in rectangular canals, using discretized boundary integral equations to solve for the velocity potential. The computational domain can be reduced to the submerged surface of the ship(s) if a Green function is used which satisfies the appropriate boundary conditions on the canal walls and bottom (and on the free surface, which is simplified in this context to a rigid flat boundary). This is in fact the motivation for the present work. In a typical application involving the interactions between two ships, each discretized with 400 panels, a linear system of dimension 800 must be set up and solved. The set-up requires the evaluation of the Green function and its gradient, for each of the $(800)^2$ combinations of the source and field point, corresponding to each element of the coefficient matrix in the linear system. These computations must be repeated for a sequence of different relative positions of the two ships, to fully describe their interactions as a function of time if one ship is passing the other. The total number of Green function evaluations is in excess of 10^7 in this case, and efficiency is clearly important. Further details of this application are presented in a separate paper [4].

In applications where Dirichlet boundary conditions are applicable the corresponding Green functions can be derived by superposition of appropriate pairs of the functions considered here, with opposite signs. Alternatively, the singly-periodic array with one

Neumann and one Dirichlet boundary condition can be evaluated from the corresponding results in [2]. (In this context a correction is required in equation (7) of [2], replacing the plus sign before the last term by \pm .)

Acknowledgement

This work has been supported by the National Science Foundation, Grant CTS-8921011.

References

1. S.R. Breit, The potential of a Rankine source between parallel planes and in a rectangular cylinder, *J. Engg. Math.* 25 (1991) 151–163.
2. J.N. Newman, The approximation of free-surface Green functions, Meeting in honour of Professor Fritz Ursell, University of Manchester, in *Wave Asymptotics*, Cambridge University Press (1991).
3. I.S. Gradshteyn and I.M. Ryzhik, *Tables of Integrals, Series and Products*, Academic Press, New York (1965).
4. F.T. Korsmeyer, C.-H. Lee and J.N. Newman, The computation of ship-interaction forces in restricted waters, submitted to *J. Ship Research*.